Available online at www.sciencedirect.com

SciVerse ScienceDirect

journal homepage: www.elsevier.com/locate/he

Hydrogen desorption from a hydride container under different heat exchange conditions

G. Andreasen [a,b,*], M. Melnichuk [c], S. Ramos [a], H.L. Corso [c], A. Visintin [a], W.E. Triaca [a], H.A. Peretti [c]

[a] Instituto de Investigaciones Fisicoquímicas Teóricas y Aplicadas (INIFTA), Facultad de Ciencias Exactas, UNLP – CONICET, CC. 16, Suc. 4, 1900 La Plata, Argentina
[b] Comisión de Investigaciones Científicas de la Provincia de Buenos Aires (CIC), Argentina
[c] Centro Atómico Bariloche – CNEA, Av. E. Bustillo 9500, 8400 S.C. de Bariloche, Río Negro, Argentina

ARTICLE INFO

Article history:
Received 16 April 2013
Received in revised form
10 July 2013
Accepted 28 July 2013
Available online 27 August 2013

Keywords:
Hydrogen storage
Metal hydride
Heat exchange

ABSTRACT

The desorption behavior of a hydrogen storage prototype loaded with AB_5H_6 hydride, whose equilibrium pressure makes it suitable for both feeding a PEM fuel cell and being charged directly from a low pressure water electrolyzer without need of additional compression, was studied. The nominal 70 L hydrogen storage capacity of the container ($T = 20\ ^\circ C$, $P = 101.3$ kPa) suffices for *ca.* 2.5 h operation of a 50 W hydrogen/oxygen fuel cell stack. The hydride container is provided with aluminum extended surfaces to enhance heat exchange with the surrounding medium. These surfaces consist of internal disk-shaped metal foils and external axial fins. The characterization of the storage prototype at different hydrogen discharge flow rates was made by monitoring the internal pressure and the temperatures of the external wall and at the center inside the container.

The response of the storage device was tested at room temperature under different conditions such as natural convection in air and forced air ventilation, and at different temperatures in a thermostated water bath, representing possible real situations to feed hydrogen/oxygen fuel cells. Current results are discussed and correlated with each particular environmental condition and hydrogen flow rate. It is found that for some environmental conditions the flow rate discharge behavior improves significantly.

1. Introduction

Hydrogen as an energy carrier has captured great interest among the scientific community and industry, particularly after the oil crisis of the 70's. The hydrogen potential as a highly energetic fuel, with pollutant-free exhaust, probably makes it the best candidate to replace hydrocarbon fuels. The requirements for the use of hydrogen as a fuel in high efficiency energy converters (as fuel cells) also comprise its production from renewable energy sources at low cost and safe and compact devices for its storage. By means of hydride forming alloys it is possible to store hydrogen from the gaseous phase within a solid structure, occupying less volume at room temperature than liquid hydrogen. Hydride formation and decomposition is a reversible process that involves a large amount of reaction heat. Hence it is important to consider the

* *Corresponding author*. INIFTA Diagonal 113 y 64, CC. 16, Suc. 4, 1900 La Plata, Argentina. Tel.: +54 221 4257291, +54 221 4257430; fax: +54 221 4254642.
E-mail address: gandreasen@inifta.unlp.edu.ar (G. Andreasen).
0360-3199/$ – see front matter
http://dx.doi.org/10.1016/j.ijhydene.2013.07.115

thermal transfer conditions from the hydride to the environment and vice versa, in order to improve the sorption process efficiency.

Considering mobile applications, a major issue still unsolved for metal hydrides is their low gravimetric density, i.e., the mass of hydrogen per mass of alloy. The U.S. DoE's targets for vehicle applications are usually taken as reference [1]. On the other hand, according to a review written by Sandrock and Bowman [2], a promising application of metal hydrides is hydrogen storage for backup systems with fuel cells. In this case, the use of AB_5-type alloys ($LaNi_5$ and its derivatives), with a hydrogen release capacity of about 1 wt%, is totally feasible.

Whatever the final application is, metal hydride beds need to be carefully designed, especially their heat exchange systems. The inherent low effective thermal conductivity of the hydride powder combined with the high heat of reaction makes it necessary to drive heat conveniently in order to reduce the reaction time to practical limits [3,4]. For this purpose, there are two main strategies: i) use of a coolant system, ii) increase of effective thermal conductivity by adding a conductive binder, or by using extended surfaces. Considering the latter option, the use of fins oriented perpendicular to the external surface of the container assures a more efficient straight heat flow in the desired direction than the use of metal foam, since the isotropic path for heat flow provided by metal foam results in a lower effective thermal conductance [5]. However, final cost, machinability and hydride volume expansion are issues that should be considered when comparing foam against fins.

Among numerous investigations related to hydrogen storage devices combined with fuel cells [6–8], the theoretical–experimental study of Jiang and co-workers [9] emphasizes the importance of using the residual heat from a PEM fuel cell in a hydride container. Their hydride model, however, considers no radial gradients, a condition that is probably the reason for slight discrepancies between numerical and experimental results.

In the present paper we carried out an experimental study on a cylindrical container, filled with AB_5H_6 hydride (equilibrium pressure ~350 kPa at 23 °C) [10], provided with internal and external fins in order to enhance the flow of reaction heat. As this container is planned to feed a laboratory size hydrogen/oxygen fuel cell stack, its performance was characterized upon discharge at constant hydrogen flow rate under different heat exchange conditions, representing the expected operative situations of a fuel cell backup system.

2. Experimental

2.1. The hydrogen container

The container used in the present work is a modified version of one reported previously [10], aimed to improve its performance associated with heat flow exchange. Its dimensions are: 50 mm outside diameter, 2 mm wall thickness and 200 mm length. It has an O-ring sealed flange at the top end, a sintered copper filter, a pressure transducer, a shutoff valve and a 1/4 in NPT connector. It is made of 304L stainless steel. The modifications introduced in the new version consisted in the incorporation of internal and external aluminum fins in order to aid heat conduction during hydrogen sorption processes.

The internal fins are disks cut out from 0.06 mm thick aluminum foil, which are located inside the container, perpendicular to its axis, as shown schematically in Fig. 1. They have a central hole that helps their positioning by a centering guide. They are mounted while loading the container with the hydride forming alloy powder, so that a stack of 60 sandwich-type layers (foil/hydride/foil) of about 2 mm width is built up. The relation between fin thickness and distance between fins was taken according to the design criterion proposed by Matsevity and co-workers [11] for a similar container. In order to allow the passage of hydrogen, the disks have needle puncture type holes with a density of about 15 holes cm^{-2}. The radii of the disks are 2 mm larger than the cylinder internal radius, and a 90° fold is applied to this extra portion of radius all around the rim, so that when the disks are inserted inside the container, they make better contact with its internal wall surface. At the same time, the folded rim defines the width of the alloy layers by keeping the distance between consecutive disks. Thus, the internal fins contribute not only to driving heat in the radial direction, but also help maintain the powder somehow confined to the space between the fins, diminishing powder compaction.

The centering guide, made of a copper tube, allows the insertion of a 1/8″ stainless steel tube with closed end, welded to the top cover flange, for the estimation of the average temperature of the hydride at the central axis of the container by means of a thermocouple.

On the other hand, 16 external longitudinal fins 30 mm wide and 150 mm long are made from two standard heat sinks as used by electronic components mechanically attached to the surface of the container. Details of the container components are shown in Fig. 2.

2.2. The hydride forming material

The material selected to fill the container is $MmNi_{4.7}Al_{0.3}$, a variant of $LaNi_5$, where Mm stands for "mischmetal", a mix of rare earths (56% Ce, 18% La, 13% Nd, 5% Pr, 2% Fe, 2% Y, 4% other rare earths). Details on the melting of this alloy and results of its characterization can be found in a previous publication [10].

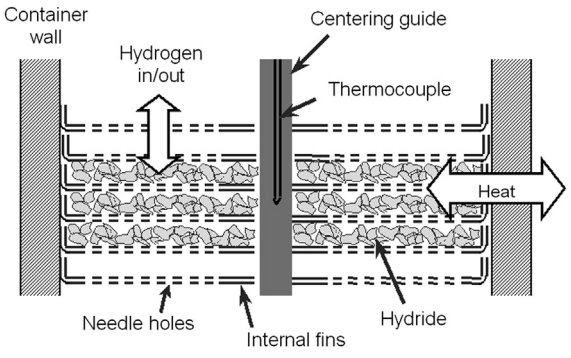

Fig. 1 – Scheme of distribution of internal fins inside the container.

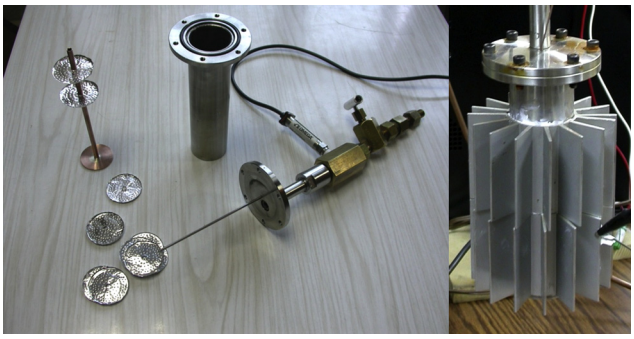

Fig. 2 – Left: storage unit components showing internal fins. Right: container assembled with external fins.

The container volume (330 cm^3) is filled with 500 ± 1.5 g of hydride forming alloy. The nominal storage capacity is of 70 L of hydrogen at 20 °C and 101.3 kPa (1atm). Taking a previously measured value of 3.5 ± 0.2 g cm^{-3} for the apparent density of the hydride powder, there is enough internal free volume for expansion of the hydride.

2.3. *Experimental setup and measurements*

Experiments consisted in monitoring the time evolution of the hydrogen dynamic pressure (P) [12], which was measured at the outlet of the storage unit, during discharges at fixed hydrogen flow rates and at constant external environment temperature (Ts). At the same time, temperatures at the center of the container (Ti) and at its external wall (Te) were also measured along the discharge using thermocouples.

The discharge measurements were performed after a previous hydrogen charge process with high-purity hydrogen (99.999%) at 2500 kPa. The container was considered charged when the hydrogen flow stopped and the container recovered its initial room temperature (20 °C), which had risen up due to the exothermic absorption reaction.

For the discharge experiments the storage unit was connected to a hydrogen-calibrated digital mass flow controller (Sierra Smart-Trak 2 Series 100), so that a constant flow rate could be established within the range 0.5–2.0 L min^{-1} (1 L min^{-1} = 4.2 × 10^{-2} mol min^{-1}). All flow rates indicated by Q are expressed in L min^{-1} and referred to room conditions ($T = 20\,^{\circ}C$, $P = 101.3$ kPa). Therefore, taking the enthalpy of hydride decomposition $\Delta H = -24.8$ kJ $mol_{H_2}^{-1}$ [13], the heat evolved per unit time in the discharge at 0.5 L min^{-1} results in 8.6 W.

Discharge measurements were carried out under different heat exchange conditions of the container: i) immersed in a water bath thermostated at either 0 °C, 20 °C or 50 °C with continuous stirring to be taken as ideal isothermal conditions (Te = Ts); ii) exposed to air, allowing for natural convection at room temperature; iii) forced convection in air along the longitudinal external fins at room temperature. This last condition was accomplished by means of a fan located below the container. The air velocity flowing around the container was estimated to be 2.5 ± 0.5 m s^{-1}. In all cases the hydride container was in vertical position, according to the design of external fins.

Due to the possibility of removing the external fins, some measurements were carried out maintaining the internal fins and without the external ones, in order to find out the relative influence of both types of fins on the thermal behavior.

For the sake of an easy understanding of the results depicted in the study we used the following nomenclature:

Heat exchange medium:
- WATER: thermostated water under stirring.
- AIR: air under natural convection condition.
- FORCED AIR: air under forced convection condition.

Container configuration subindex:
- No fins: configuration of the container without fins.
- Int fins: container with internal disk-shaped fins and without external fins
- Ext–Int fins: container with external and internal fins.

All discharge measurements were stopped according to an adopted cutoff criterion, consisting in preventing the gauge pressure from becoming lower than 125 kPa. The purpose of this was to avoid the entrance of atmospheric gases into the container.

In order to check the storage capacity of the container, the hydrogen absorbed during the charge was measured employing the mass flow controller. As a result, both hydrogen charge and discharge values were consistent and in agreement with the indicated nominal storage capacity.

3. Results and discussion

3.1. *Pressure evolution along discharges at 0.5 L min^{-1} and 20 °C*

The container was tested for a hydrogen desorption flow rate according to its design condition, i.e., 0.5 L min^{-1} at room conditions (20 °C and 101.3 kPa). However, additional tests were also performed at 2.0 L min^{-1} for the sake of characterizing the storage prototype behavior for heavy-duty conditions.

In order to evaluate the effect of the internal and external fins on the container performance, the present results are compared with previous ones obtained in a similar container without fins, reported in [14], where numerical simulations and experimental results, including a sensitive analysis of the main associated physical parameters, were used to characterize the system under study.

In Fig. 3 a plot of the hydrogen dynamic pressure as a function of time corresponding to discharges at 0.5 L min^{-1} is shown. The measurements were carried out with the container either under water or exposed to air at Ts = 20 °C. In both cases, results of the container equipped with different fin configurations are shown for comparison.

A general feature of the curves is a pronounced initial pressure drop, corresponding mainly to the release of the compressed hydrogen gas inside the container, until a smooth pressure decrease is attained, which constitutes a "dynamic plateau" due to hydride decomposition.

It can be observed that the discharge curves corresponding to $WATER_{No\ fins}$ and $WATER_{Ext-Int\ fins}$ configurations almost

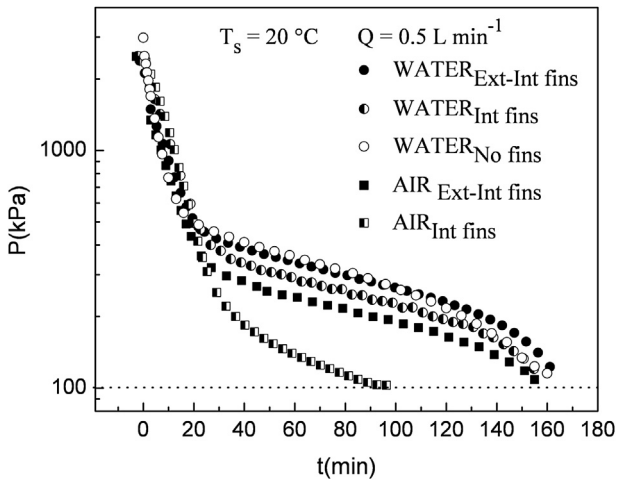

Fig. 3 – Dynamic pressure as a function of time for different container configurations and environment conditions at 0.5 L min^{-1} discharge flow rate. The dotted line indicates the cutoff pressure.

overlap, practically releasing a similar amount of hydrogen. Considering the high efficiency of stirred water to exchange heat, it can be inferred that, for this discharge flow rate and environment condition, the global reaction rate is mainly controlled by the heat transfer through the metal hydride inside the container, independently of the presence of internal and external fins. This fact is corroborated by the similar behavior of the discharge curve obtained at WATER$_{Int\ fins}$, which desorbs almost the same amount of hydrogen in spite of a small decrease of the dynamic pressure. This would also imply a small influence of internal fins for the considered flow rate and environment conditions in this case.

The amount of recovered hydrogen stored as hydride can be estimated by calculating the amount of released gas along the "dynamic plateau". Considering the duration of the discharge of this plateau from about 20 to 160 min, the recovered hydrogen flowing at 0.5 L min^{-1} (6.9×10^{-4} g s^{-1}) for 140 min is *ca.* 70 L.

It is worthwhile to note that since the energy storage density for hydrogen is 142×10^3 J g^{-1}, this flow rate of 6.9×10^{-4} g s^{-1} is equivalent to 98 W power delivery, which would be enough to feed a 50 W hydrogen/oxygen PEM fuel cell operating at maximum power for 140 min. For the estimation of this fuel cell power value it has been considered that the maximum electrical energy available is equal to the change in Gibbs free energy (ΔG) for the fuel cell reaction, so

$$\text{Maximum efficiency} = (\Delta G/\Delta H)\ 100\% \quad (1)$$

where ΔH is the reaction enthalpy change, that is, the total energy available in the process. Since ΔG is less than ΔH because of the reaction entropy change, which generates heat rather than electricity, the maximum efficiency at 20 °C is *ca.* 82%. In addition, all other heat losses related to the irreversibility of cell reactions should also be taken into account as they diminish the fuel cell practical efficiency to *ca.* 50%–55%, yielding, therefore, a maximum power output of about 50 W.

On the other hand, for the case of the operation in air, a different behavior takes place between AIR$_{Ext-Int\ fins}$ and AIR$_{Int\ fins}$ configurations. In both cases the dynamic pressure decreases, and this effect is more pronounced in the AIR$_{Int\ fins}$ case, as expected due to the less heat transfer efficiency through the container wall by air convection. For AIR$_{Ext-Int\ fins}$, the amount of recovered hydrogen is 68 L, which is approximately the same as when the container is immersed in water, while for AIR$_{Int\ fins}$ this amount considerably diminishes to 40 L (Table 1). This behavior can be understood in terms of the lowering of the hydride temperature due to a less efficient heat transfer, giving rise to a decrease of the dynamic pressure and hence a sooner arrival at the cutoff pressure (dotted line in Fig. 3).

A comparison of the container performance under FORCED AIR$_{Ext-Int\ fins}$ and WATER$_{Ext-Int\ fins}$ conditions at 0.5 L min^{-1} and 20 °C shows similar behavior in both cases (Fig. 4). However, the use of forced air in the finned configuration implies an extra energy consumption of about 12 W. This should be considered when evaluating the convenience of using forced air or water immersion as heat exchanging media for the container during hydrogen sorption reaction.

3.2. *Pressure evolution along discharges at 2.0 L min^{-1} and 20 °C*

Hydrogen discharge curves at a flow rate of 2.0 L min^{-1} from the container equipped with different fin configurations and exposed either to air or immersed in water at Ts = 20 °C are shown in Fig. 5.

It can be observed that for the WATER$_{Ext-Int\ fins}$ case, the dynamic plateau of the discharge runs from 7 to 42 min. This represents *ca.* 70 L of recovered hydrogen, which is the same amount obtained at 0.5 L min^{-1}. On the other hand, for WATER$_{No\ fins}$ the discharge at 2 L min^{-1} runs from 7 to 31 min, resulting in only 48 L of recovered hydrogen (Table 1). This can also be understood because of the decrease of the dynamic pressure and sooner arrival at the cutoff pressure. Hence, for the operation under water at 2 L min^{-1}, an improvement in discharge capacity of about 45% is obtained due to the presence of fins.

For the WATER$_{Int\ fins}$ case, the discharge runs from 7 to 41 min. This is equivalent to *ca.* 68 L of recovered gas, representing approximately 97% of the recovery when compared to the WATER$_{Ext-Int\ fins}$ condition (Table 1). In this case, the improvement due to the use of internal fins is about 40% with respect to the WATER$_{No\ fins}$ case. This clearly shows that at a

Table 1 – Recovered hydrogen for the different discharge conditions at 20 °C.

Configuration	Flow rate	
	0.5 L min^{-1}	2 L min^{-1}
WATER$_{No\ fins}$	70 L	48 L
WATER$_{Int\ fins}$	70 L	68 L
WATER$_{Ext-Int\ fins}$	70 L	70 L
AIR$_{Int\ fins}$	40 L	10 L
AIR$_{Ext-Int\ fins}$	68 L	26 L

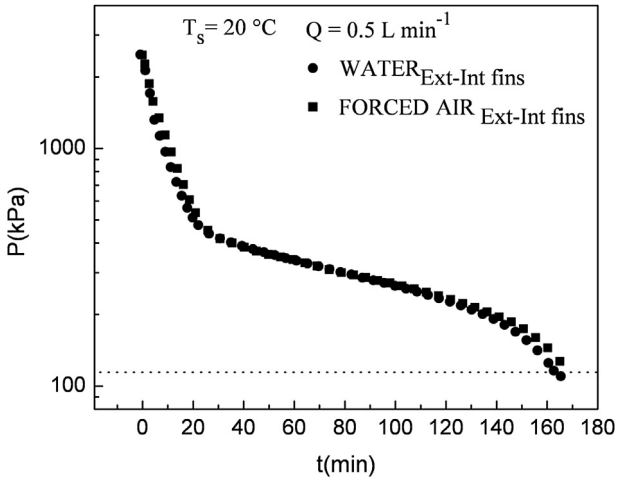

Fig. 4 – Container performance under WATER$_{Ext-Int\ fins}$ and FORCED AIR$_{Ext-Int\ fins}$ conditions. The dotted line indicates the cutoff pressure.

flow rate of 2.0 L min^{-1}, the internal fins play an important role, which is different to the behavior observed at the slower flow rate of 0.5 L min^{-1}. This result also suggests that contact resistance of the disk-shaped internal fins is not a major issue.

Regarding the behavior when the stored hydrogen is discharged at 2.0 L min^{-1} with the container exposed to air, it can be seen from Fig. 5 that a performance improvement of about 160% is found for the AIR$_{Ext-Int\ fins}$ condition when compared to AIR$_{Int\ fins}$. This fact reveals the relevance of heat transfer through the external walls at this flow rate when operating in air.

3.3. *Temperature evolution along discharges at 0.5 L min^{-1}*

Fig. 6 shows the time evolution of internal and external container temperatures (denoted as Ti and Te, respectively)

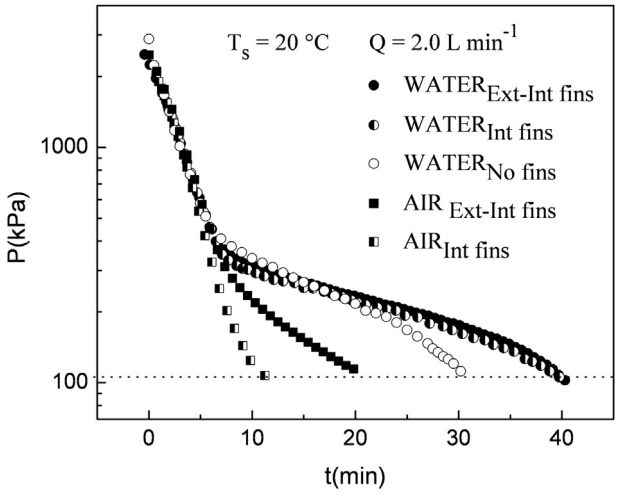

Fig. 5 – Dynamic pressure as a function of time for different container configurations and environment conditions at 2.0 L min^{-1} discharge flow rate. The dotted line indicates the cutoff pressure.

measured during discharge experiments at 0.5 L min^{-1} under different environments (water or air at Ts = 20 °C). The temperatures Ti and Te correspond to the same set of measurements that is shown in Fig. 3. It can be observed that, except for Te corresponding to the isothermal case with water at 20 °C (dashed line), in all other cases, Ti and Te show an initial decrease after which they tend to stabilize remaining almost constant, constituting a quasi-stationary regime.

For the case of the container immersed in water at 20 °C, Ti presents a decrease of about 3.5 °C with respect to Te for both WATER$_{Ext-Int\ fins}$ and WATER$_{Int\ fins}$ conditions. This behavior is also consistent with the previous observation that for the container in water, the presence or absence of external fins does not make any difference in the heat transfer through the container wall when discharging at 0.5 L min^{-1}. The temperature attained by the hydride at the center of the container is the same, and the temperature difference between the center and the external wall is proportional to the heat flow in the radial direction.

On the other hand, for AIR$_{Ext-Int\ fins}$, a lowering of about 5.5 °C in the external fin temperature (Te) with respect to environment temperature (20 °C) occurs, indicating that heat transfer by convection through the external surface is less than in the WATER$_{Ext-Int\ fins}$ case. Ti also presents a decrease of about 4.5 °C with respect to Te, corresponding to the heat flow in the radial direction. In this case, the temperature difference is somewhat larger than in the case of operation in water.

For the case of AIR$_{Int\ fins}$, a continuous temperature lowering is observed during the whole discharge, with Ti down to −4 °C and Te to 0 °C, where the same kind of quasi-stationary regime seems to begin.

It can be pointed out that the temperature lowering in all the cases operating in air is larger than in the case of operation in water, as a result of the lower heat transfer through the external container surface by convection and therefore Te should be related to heat transfer with the surrounding medium. On the other hand, the temperature difference Δ(Te−Ti) of the quasi-stationary regime in all cases results of the same order, between 3.5 °C and 5.5 °C. This can be understood in terms of a similar heat evolution, given by the same discharge flow rate at 0.5 L min^{-1}.

3.4. *Temperature evolution along discharges at 2.0 L min^{-1}*

As shown in Fig. 7, when the hydrogen storage device is operated at a discharge rate four times faster, i.e., 2.0 L min^{-1}, a decrease of both Te and Ti takes place in all cases, except for Te corresponding to the isothermal case with water under stirring at 20 °C (dashed line). For the operation in air, the temperature lowering is more pronounced and no quasi-stationary regime can be attained before the end of the discharge. However, when the container is immersed in water, after 10 min of initial drop, a quasi-stationary regime occurs, where temperature continues decreasing at a slow rate for another 30 min until the end of the discharge, in agreement with Fig. 5. As expected, due to the high heat transfer between water and the container wall, the external fins do not play a key role. However, the presence of internal

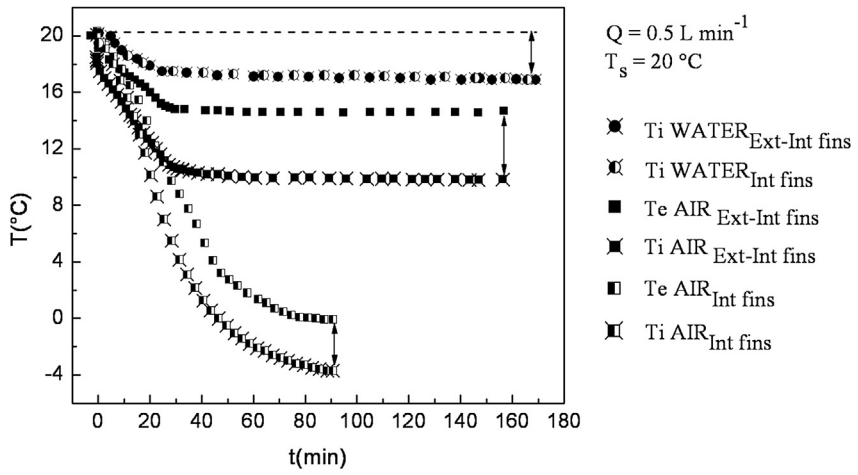

Fig. 6 – Evolution of internal and external container temperatures for different finned configurations and environment conditions at 0.5 L min^{-1} discharge flow rate. The dashed line corresponds to the isothermal condition (Te = Ts).

fins allows an important improvement in the amount of recovered hydrogen, as pointed out in 3.2.

The comparison between $AIR_{Ext-Int\ fins}$ and $AIR_{Int\ fins}$ cases shows an important rise of Ti and Te due to the presence of external fins. A remarkable difference between Ti and Te is observed in both cases, as occurs when the discharge flow rate is 0.5 L min^{-1}. But here, the difference at the end of the discharge is twice as much due to the higher flow rate.

3.5. *Pressure evolution along discharges at 0.5 L min^{-1} and different temperatures*

The dynamic pressure evolution upon discharges at 0.5 L min^{-1} flow rate for the $WATER_{Ext-Int\ fins}$ condition at temperatures of 0 °C, 20 °C and 50 °C is shown in Fig. 8. In the discharge curve at Ts = 50 °C, the end of the dynamic plateau pressure can be identified by a second pressure drop, before the end of the discharge determined by the cutoff pressure. This seems to be a consequence of the fact that equilibrium pressure increases and the plateau width becomes narrower on temperature increase. Hence, the arrival at the cutoff pressure that determines the stop of the discharge takes place after the end of the dynamic plateau.

For discharges at lower temperatures, the extension of the dynamic pressure plateau becomes larger, but only the part that is above the cutoff pressure can be seen in the discharge curve, as is the case of the measurements at 20 °C and 0 °C, where the end of the plateau does not show up.

From these results, despite the higher equilibrium pressure at 50 °C, the discharge at 20 °C with a flow rate of 0.5 L min^{-1} is the more convenient to maximize the amount of hydrogen to be recovered.

4. Summary of results

Results obtained from the dynamic pressure evolution at 0.5 L min^{-1} operating in water under stirring show that the incorporation of fins is irrelevant because the heat flow is controlled by the hydride bulk. At this discharge rate, the

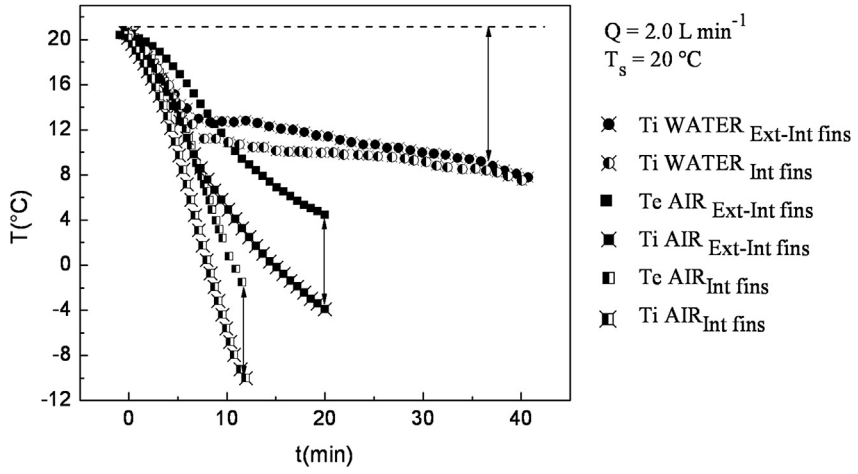

Fig. 7 – Evolution of internal and external container temperatures for different finned configurations and environment conditions at 2.0 L min^{-1} discharge flow rate. The dashed line corresponds to the isothermal condition (Te = Ts).

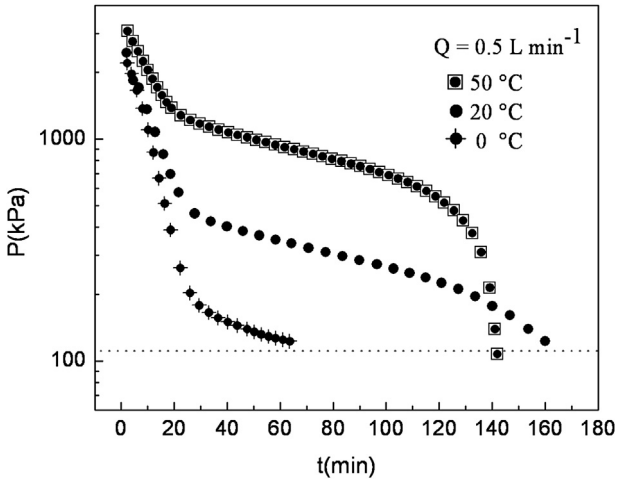

Fig. 8 – Dynamic pressure as a function of time for different environment temperatures at 0.5 L min^{-1} discharge flow rate. The dotted line indicates the cutoff pressure.

amount of released hydrogen is *ca.* 70 L (discharge time: 140 min), approaching the nominal container storage capacity. However, the beneficial effect of internal fins operating in water at 2.0 L min^{-1} and Ts = 20 °C should be noted.

On the other hand, for the other conditions shown in Table 1, the effect of external fins appears as an improvement of the discharge capacity. For instance, at 0.5 L min^{-1} in AIR$_{\text{Ext–Int fins}}$, a slight decrease of the dynamic pressure occurs as compared to WATER$_{\text{Ext–Int fins}}$, whereas this decrease is significantly larger in AIR$_{\text{Int fins}}$, due to the lower heat transfer efficiency.

Thus, the efficiency of a particular container configuration, i.e., with or without fins, should be evaluated for fixed external conditions (temperature and heat exchange environment). A clear example is provided by the results obtained for discharge at 0.5 L min^{-1} and 20 °C for FORCED AIR $_{\text{Ext–Int fins}}$. The comparison between this condition and WATER$_{\text{Ext–Int fins}}$ does not show a significant improvement of the discharge performance. Hence, the convenience of forced air operation should be evaluated considering the extra energy consumption of the fan and the availability of heating water or air flow.

The analysis of the temperature evolution shows an initial steep decrease in all internal and external container temperatures (Ti and Te), with the exception of the WATER$_{\text{Ext–Int fins}}$ case, where Te attains the ideal isothermal condition by the use of an external stirring system. For other cases, after the initial decrease, a quasi-stationary regime follows, where the temperature remains almost constant. This temperature becomes lower as external fins are removed, due to a decrease of heat thermal efficiency. The temperature difference Δ(Te–Ti) of the quasi-stationary regime for a given flow rate is of the same order, while the final temperature is related to the container configuration.

For discharges at 2 L min^{-1} with the container in air, Ti and Te show a pronounced decrease until the end of the discharge without presenting a quasi-stationary regime for all different finned configurations. The difference Δ(Te–Ti) in these cases is of the order of 8 °C at the end of the discharge, due to the higher discharge flow rate leading to higher temperature gradients within the container.

It should be noted that for the WATER$_{\text{Ext–Int fins}}$ case at the design working flow rate of 0.5 L min^{-1} and Ts of 0 °C, 20 °C and 50 °C, the most appropriate temperature to get the maximum amount of recovered hydrogen is 20 °C (see 3.5).

5. Conclusions

A hydrogen storage prototype was constructed presenting a good performance to recover hydrogen from the metal hydride decomposition at the design working conditions, i.e., capable of delivering 70 L of hydrogen at 0.5 L min^{-1} and 20 °C, in order to feed a 50 W hydrogen/oxygen PEM fuel cell for 140 min. This satisfactory behavior is achieved for any finned container configuration, even in the absence of fins, when the container is immersed in a thermostated water bath, while when exposed to air it requires to be equipped with external fins.

Discharges at a higher hydrogen flow rate, namely 2 L min^{-1}, with finned container configurations and different heat exchange media were also performed. The results show that under these conditions, the amount of released hydrogen approaches the nominal container storage capacity by operating in water at 20 °C under stirring.

The use of internal and external fins improves, as expected, the heat transfer by diminishing thermal gradients. This leads to a less lowering of the dynamic pressure and consequently to an increase of the discharge capacity.

Acknowledgments

This work had the financial support of the following Argentinian institutions: CONICET, CNEA and ANPCyT. G. Andreasen is a member of the research career of the Comisión de Investigaciones Científicas de la Provincia de Buenos Aires (CIC).

REFERENCES

[1] Satyapal S, Petrovic J, Read C, Thomas G, Ordaz G. The U.S. department of energy's national hydrogen storage project: progress towards meeting hydrogen-powered vehicle requirements. Catalysis Today 2007;120:246–56.
[2] Sandrock G, Bowman Jr RC. Gas-based hydride applications: recent progress and future needs. Journal of Alloys and Compounds 2003;356–357:794–9.
[3] Gadre SA, Ebner AD, Al-Muhtaseb SA, Ritter JA. Practical modeling of metal hydride hydrogen storage systems. Industrial and Engineering Chemistry Research 2003;42:713–1722.
[4] Gadre SA, Ebner AD, Ritter JA. Two dimensional model for the design of metal hydride hydrogen storage systems. Adsorption 2005;11:871–6.
[5] Mosher DA, Arsenault S, Tang X, Anton DL. Design, fabrication and testing of $NaAlH_4$ based hydrogen storage systems. Journal of Alloys and Compounds 2007;446–447:707–12.
[6] Brown TM, Brouwer J, Samuelsen SG, Holcomb FH, King J. Accurate simplified dynamic model of a metal hydride

tank. International Journal of Hydrogen Energy 2008;33:5596–605.
[7] Brown TM, Brouwer J, Samuelsen GS, Holcomb FH, King J. Dynamic first principles model of a complete reversible fuel cell system. Journal of Power Sources 2008;182:240–53.
[8] Guizzi GL, Manno M, De Falco M. Hybrid fuel cell-based energy system with metal hydride hydrogen storage for small mobile applications. International Journal of Hydrogen Energy 2009;34:3112–24.
[9] Jiang Z, Dougal RA, Liu S, Gadre SA, Ebner AD, Ritter JA. Simulation of a thermally coupled metal-hydride hydrogen storage and fuel cell system. Journal of Power Sources 2005;142:92–102.
[10] Melnichuk M, Andreasen G, Corso HL, Visintin A, Peretti HA. Study and characterization of a metal hydride container. International Journal of Hydrogen Energy 2008;33:3571–5.
[11] Matsevity M, Solovey V, Chernaya N. In: Proceedings of the world hydrogen technologies convention WHTC 2007 2007. Montecatini Terme, Italy.
[12] Goodell PD, Sandrock GD, Huston EL. Kinetic and dynamic aspects of rechargeable metal hydrides. Journal of the Less Common Metals 1980;73:135–42.
[13] Rodríguez D. Thesis Work. Balseiro Intitute-U.N.C./C.N.E.A.; 2000.
[14] Melnichuk M, Silin N, Andreasen G, Corso HL, Visintin A, Peretti HA. Hydrogen discharge simulation and testing of a metal-hydride container. International Journal of Hydrogen Energy 2010;35:5855–9.